

Open-access microfluidic patch-clamp array with raised lateral cell trapping sites†

Adrian Y. Lau, Paul J. Hung, Angela R. Wu and Luke P. Lee*

Received 14th June 2006, Accepted 7th September 2006

First published as an Advance Article on the web 27th September 2006

DOI: 10.1039/b608439g

A novel open-access microfluidic patch-clamp array chip with lateral cell trapping sites raised above the bottom plane of the chip was developed by combining both a microscale soft-lithography and a macroscale polymer fabrication method. This paper demonstrates the capability of using such an open-access fluidic system for patch-clamp measurements. The surface of the open-access patch-clamp sites prepared by the macroscale hole patterning method of soft-state elastic polydimethylsiloxane (PDMS) is examined; the seal resistances are characterized and correlated with the aperture dimensions. Whole cell patch-clamp measurements are carried out with CHO cells expressing Kv2.1 ion channels. Kv2.1 ion channel blocker (TEA) dosage response is characterized and the binding activity is examined. The results demonstrate that the system is capable of performing whole cell measurements and drug profiling in a more efficient manner than the traditional patch-clamp set-up.

Introduction

Patch-clamp recording has been the major research tool for electrophysiology. Information obtained from ion channel current measurements has significant implications on drug target identification.¹ Developed by Erwin Neher and Bert Sakmann in 1976,² patch-clamping involves using a conductive fluid-filled glass micropipette to contact and form a high resistance seal with a cell. Through the electrodes in the micropipette and in the cell buffer solution, current measurement can be taken with the voltage fixed (voltage-clamp configuration). Since the cell membrane potential is directly related to the ion transfer through the membrane, functional information on ion flux into or out of the cell can be obtained from the current data. Despite the usefulness of the method, the process is labor intensive, time consuming and low throughput for applications such as drug discovery, quantitative biology and molecular medicine. Micropipette handling for patch-clamping requires highly trained professionals and is time-consuming; in a day a typical expert technician might clamp a maximum of 15 cells.³

The inherent complexity of the technique limits its uses in high throughput screening for drug discovery and drug safety, and has fueled the development of chip-based devices in an attempt to automate the technique for parallel operations.¹ Planar patch-clamp arrays made of silicon,⁴ silicon nitride,⁵ glass,^{6,7} polyimide,⁸ and silicone elastomer^{9,10} have been demonstrated; however, the overall system is expensive because complicated fabrication methods are required for the fluidic interface. In addition, most of the above methods are not compatible with high magnification optical microscopy because the overall device is too thick for imaging with short working distances. There is also a limitation on

the density of the aperture placement due to the complexity of the fluidic interface. A planar patch-clamp approach is therefore inefficient when used for single-cell level studies that require simultaneous high-resolution imaging and current measurement. A lateral patch-clamp made from polydimethylsiloxane (PDMS) elastomer using a soft lithography technology¹¹ was shown to be advantageous due to the simple and low cost fabrication steps, straightforward fluidic integration, the transparent property of the material and the capability to have close patch aperture placement.^{12,13} Moreover, the lateral-based patch-clamp set-up is compatible with high resolution microscopy (with a working distance in the 100–300 μm range). The idea is to trap a cell onto a lateral microchannel in a manner which makes it easier in terms of fabrication and fluidic integration.^{12–14} However, previous studies^{12,13} based on these PDMS lateral patch-clamp devices show substandard seal quality formation with cells, with seal resistances measured at around 150 M Ω –250 M Ω ; moreover, the trapping sites which are contacting the bottom plane of the chip give the patched cell an uncommon deformation, whereas its impact on cellular response is still not clear. In addition, the enclosed microscale fluidic chamber poses a problem when efficient fluidic exchange and minimal seal quality perturbation are required; the low Reynold's number of the fluid in the microscale chamber limits the diffusion rate. Thus in a microscale volume it is difficult to efficiently perfuse a specific concentration of drug to the cell at a low flow rate while keeping the patched area of the cell intact.

We present here a novel patch-clamp array with the cell trapping locations “raised” above the bottom plane of the chip to better resemble traditional glass micropipette openings. The main fluidic chamber is open to the air, providing an easy-to-use platform for fluidic exchange. Seal resistances were characterized with mammalian HeLa cells and the optimum patch aperture dimensions were determined. Extensive whole cell patch-clamp experiments were performed on CHO cells expressing Kv2.1 ion channels, including ion channel I–V correlation, drug dose–response, and drug binding activity

Biomolecular Nanotechnology Center, Berkeley Sensor & Actuator Center, Department of Bioengineering, University of California-Berkeley, Berkeley, CA 94720 E-mail: lplee@berkeley.edu; Fax: +1 (510)642-5835; Tel: +1 (510)642-5855

† The HTML version of this article has been enhanced with additional colour images

characterizations. The result demonstrates that this platform is suitable for high throughput electrophysiology research and development, and provides an easy transition from the traditional patch-clamp approach.

Device design

One major concern over previous lateral patch-clamp designs is that of the geometry of the structure, where the patch channel is lying on a flat substrate.¹² This gives unnatural deformations to the cells when they are being trapped at the trapping site (Fig. 1(a)). The proposed method circumvents the problem by combining a regular PDMS microdevice processing method with a macroscale punching approach which will be described in detail in the fabrication section. The channel opening created with this method is raised above the flat substrate, giving a patching site comparable to the traditional micropipette setting (Fig. 1(b)). Since the macroscale punching step creates a large chamber open to the air, it can also be used as a solution exchange site. Fig. 1(c) shows the device at an angled view, and demonstrates how solution can be supplied into the open chamber simply through a pipette tip. The open access chamber is also compatible with the common solution perfusion set-up developed for traditional patch-clamp. In fact, most equipment set-up described here is similar to the traditional patch-clamp set-up. The major difference is that instead of interfacing the electrode to a glass micropipette, the electrode is interfaced through PTFE tubing to the device. This simplifies the patch-clamp system architecture by eliminating all the micromanipulation tools and the requirement for a vibration-free environment.

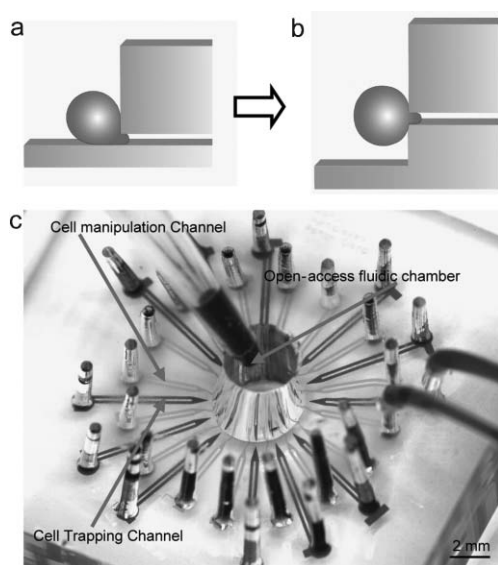


Fig. 1 (a) Cross-sectional illustration showing how the cell is trapped in the previous lateral patch-clamp device.^{12,13} (b) Cross-sectional illustration showing how the cell is trapped in the device discussed in this paper. (c) Angled view of the device. Patch channels and cell manipulation channels were filled with two different dyes. The open-access chamber is shown in the image, where cells or drug samples can easily be pipetted in.

Fabrication

The main PDMS microfluidic channels part is fabricated with a conventional soft lithography procedure. Briefly, the structures are created on a silicon wafer *via* a lithography process with SU-8 (SU-8 2002 and SU-8 2050, MicroChem) photoresist. After the mold is completed, PDMS (Sylgard 184, Dow Corning) prepolymer is mixed (10 : 1) and cast on the mold and cured. The cured PDMS is then peeled and cut out. Small holes (~ 0.5 mm) for fluidic connection are created with a hole punching kit (Technical Innovations). A 20 μm layer PDMS membrane is prepared by spin-coating PDMS prepolymer on a new silicon wafer coated with Omnicore (MicroChem) at 4000 rpm. The PDMS device piece is then bonded to the PDMS membrane by treating both surfaces with the oxygen plasma. After bonding, the device together with the membrane is peeled off from the silicon wafer. A custom-made hole punching set-up is put together by combining a 4 mm OD punching pin (Technical Innovations), a table-top drill press (GMC), and a microscope (Olympus MIC-D). The set-up ensures uniformly punched holes and allows punching alignment with an accuracy of ± 50 μm . The set-up is used to punch the center chamber of the device. The device is then bonded onto a glass slide and is ready to use. The complete fabrication procedure is summarized in Fig. 2.

Cell culture

HeLa cells and Chinese hamster ovary (CHO) cells are used for experiments. For HeLa cells the cells are cultured till 80%–90% confluency in Dulbecco's Modified Eagle's Medium (DMEM, Gibco) with 10% Fetal Bovine Serum (FBS, Gibco). To harvest the cells, the cells are first rinsed with Phosphate-Buffered Saline (PBS, Gibco) and then incubated in Trypsin (Gibco) for 5 min at 37°. DMEM with FBS is added to neutralize the Trypsin. The cells are then aspirated and centrifuged. After the centrifugation the media is replaced with PBS solution and the cells are ready to use. The cell

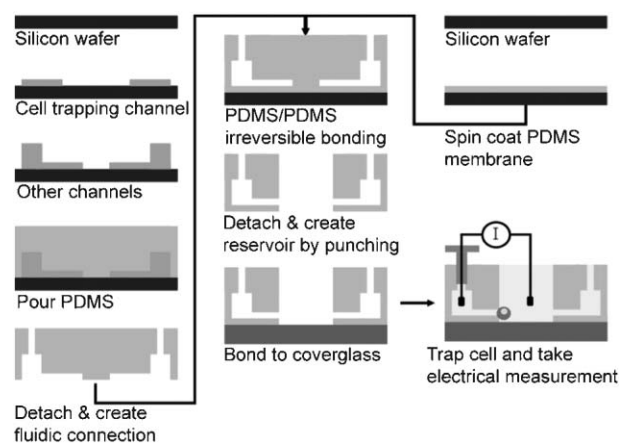


Fig. 2 Fabrication of the device. The novelty in this fabrication process is that the melded PDMS channel is bonded onto a thin PDMS membrane. Afterwards a 4 mm OD hole-puncher is cut through the device vertically, opening up the micro-channels while creating an open-access fluidic chamber.

concentration in the suspension is around 1×10^6 cells ml^{-1} . The CHO cells used for experiments are transfected with Kv2.1 potassium ion channels with a tetracycline induced expression vector.¹⁵ The cells are cultured till 80%–90% confluency in DMEM with 7.5% FBS. $4 \mu\text{g ml}^{-1}$ Tetracycline (or $2 \mu\text{g ml}^{-1}$ Doxycycline) is added to the culture media 12 h before experiment to induce Kv2.1 expression. The cells are harvested the same way as the HeLa cells described above, but the cells are resuspended in an electrolyte buffer solution before use. The electrolyte buffer solution consists of (in mM): 140 KCl, 2 CaCl₂, 2 MgCl₂, 20 HEPES, and 10 glucose. The pH is adjusted to 7.3 with KOH and the osmolality is adjusted to 300 mOsm with glucose. The intracellular and extracellular solution in the whole cell patch-clamp experiments are the same buffer solution. For cell labelling, Calcein AM, Hoechst 33258, and R18 (Molecular Probes) are used.

Set-up and device operation

All the electrical measurements are done inside a faraday cage (TMC) to isolate the electromagnetic interference from the 60 Hz wall plug and the outer environment. All fluidic connections are made by inserting PTFE tubing (Cole Parmer) into the punched holes. Patch-clamp electrode holders and Ag/AgCl electrodes are purchased from Warner Instruments. Tubings are fitted into the electrode holder and connected to 3 ml syringes. The electrodes are connected to the headstage of the patch-clamp amplifier (Dagan Corporations), and the amplifier is controlled by a computer interface (NI-6024E, National Instruments) *via* Labview programs (National Instruments).

Before the experiment, all the syringes are filled with buffer solution. The tubing connected to the main electrode is plugged into the patch channel, while the tubing connected to the reference electrode is plugged into the reference channel (Fig. 3(a)). The device is then filled with the buffer solution. Since PDMS is gas permeable, pressure is applied to the inlets to eliminate any bubbles inside the microfluidic device. Cell suspensions are then loaded in a 3 mL syringe and flowed into the device through the cell introduction channel (Fig. 3(b)). Pressure on the cell introduction channel can be manipulated to move the cells around until a target cell is close to the patch opening (Fig. 3(c)). Negative pressure is applied on the cell trapping channel and the cell will get “patched” (Fig. 3(d)). When the cell is “patched”, the resistance will rise and saturate at a certain level. High resolution imaging (with a Zeiss 100 \times oil immersion objective lens) of the deformation of the cell is obtained after trapping it onto a patch channel in Fig. 3(e), (f).

Results and discussion

Macroscale fabricated surface

One major concern over the fabrication method described here is that the use of the macroscale punching method might generate a rough surface which would reduce the surface compatibility and thus the seal quality. SEM images of the patch aperture (Fig. 4(a), (b)) confirm that the surface is smooth and that the aperture is indeed raised above the glass substrate. One important note about the fabrication method is

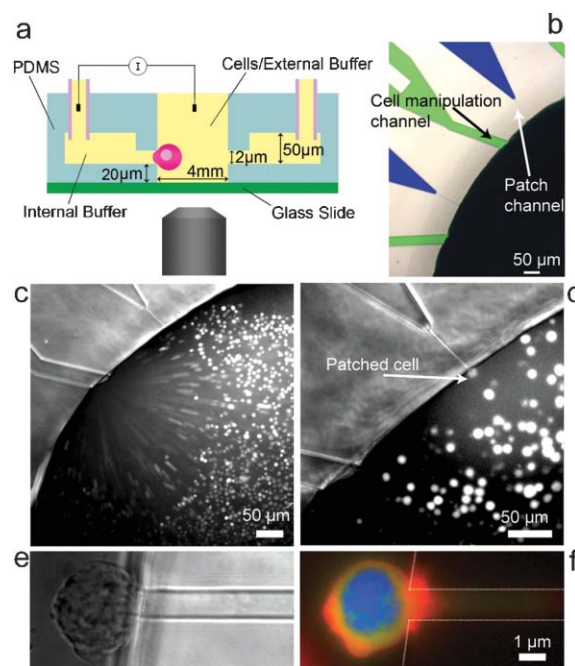


Fig. 3 (a) Schematic of the set-up showing how the cell is being trapped onto the channel from a cross-sectional view. (b) Close-up image of the channels of the devices—small patch channel for trapping cells and larger channel for cell manipulation. (c) Long exposure image of cells being manipulated *via* the wide channel. The manipulation channel allows cells to be brought close to the patch channel. The cells were dyed with calcein AM. (d) Image showing a cell being trapped and patched on the small channel. (e) Close-up of a trapped cell on the patch channel in bright field. (f) Fluorescent image of the same cell in (d). The cell is stained with calcein AM (cytoplasm, green), R18 (membrane, red), and Hoechst (nucleus, blue).

that the macroscale punching step generates a reasonable amount of force onto the channels, and sometimes this force would cause the small patch channels to collapse and thus seal up the opening. Three steps are identified to minimize the problem. Firstly, the small patch channel on the mold should have an aspect ratio of at most 1 : 1, *i.e.* the height of the channel should be equal or longer than the width. Secondly, after bonding the PDMS channels onto the membrane with oxygen plasma, the device should be left alone for 24 h before carrying out the punching step. This is to make sure that the charged surface is neutralized so that irreversible bonding will not occur even if the channels are pressed down. Thirdly, the hole puncher fixed on the drill press must be pressed down gently and slowly while punching the center hole.

Seal resistance characterization

To continuously monitor the resistance change, a labview (National Instruments) program is used to apply square pulses with amplitudes of 10 mV at a bias voltage of -60 mV with a frequency of ~ 130 KHz. The current response is divided by the applied voltage to obtain the equivalent resistance. Before any cell is trapped onto the patch channel, a resistance measurement is taken that is denoted as the open channel resistance (R_{open}), which is the resistance of the circuitry plus the fluidic resistance. Once a cell is trapped, the seal resistance

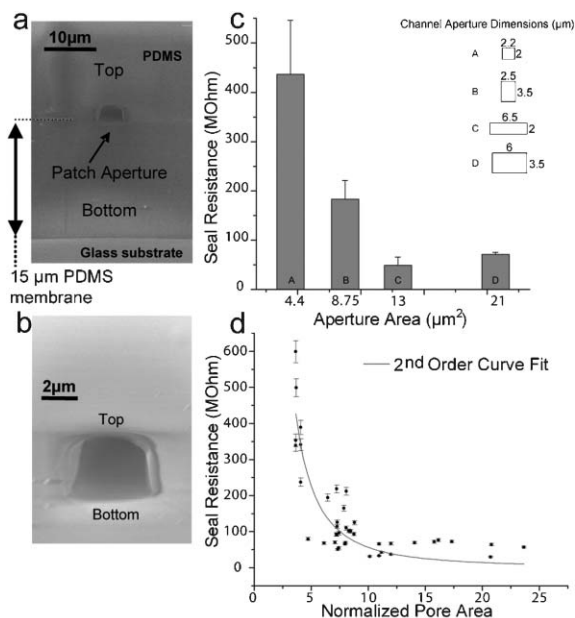


Fig. 4 (a)–(b) SEM of the raised patch aperture. (c) Seal resistance characterization with 4 different patch apertures. (d) Characterization of seal resistance dependence on patch aperture size. The patch aperture area is determined from normalization of the channel length over the open channel resistance.

(R_{seal}) can be calculated by deducting the open channel resistance from the resistance measurement at that time. Seal resistances are observed after a cell is trapped onto the patch channel. HeLa cells are used for seal resistance characterization because they form a relatively stable seal and have a smaller seal resistance variation from cell to cell when compared to CHO cells or NIH3T3 cells. In order to determine the optimum aperture dimensions that would give the best quality seal resistance, patch apertures with different dimensions are fabricated. As shown in Fig. 4(c), patch channels with four different dimensions are fabricated and tested (the dimensions are obtained by taking SEM images of the mold). The results show that in general a smaller aperture substantially increases the seal resistance. One point to note is that although geometry *D* is larger in area than geometry *C*, the results show better seal performance for geometry *D*. The reason we believe is that *D* has a width/height ratio closer to 1 than *C* (*i.e.* *D* is more “square” than *C*), and it is easier for the cell to deform to fill up a “square” aperture than a “rectangular” aperture, which leads to the better seal performance in *D* than in *C*. To further characterize seal resistance, the exact aperture size of each channel is determined. When no cell is present, the resistance of the small patch makes up for most of the resistance in the system since its cross-sectional area is significantly smaller than the rest of the system. Hence it can be safely assumed that the open channel resistance is proportional to the length of the patch channel divided by the cross-sectional area of the channel defined as:

$$\text{Aperture Area} = K \frac{\text{Channel Length}}{R_{\text{open}}}$$

With the equation the aperture area can be obtained simply by measuring the R_{open} and the channel length. (The constant K is determined from a channel with known aperture area.) Fig. 4(d) shows a plot of the seal resistance against the aperture area determined from the equation above. The plot shows an exponential relationship, and a 2nd order curve is fitted to the results, yielding the relation (R^2 value = 0.76):

$$R_{\text{seal}} = \frac{b}{A_{275}^2} \quad b = 5647.9 \quad A = \text{Aperture Area}$$

Since the results show that a smaller channel is better in forming high seal resistance, a device with a $2 \mu\text{m} \times 2 \mu\text{m}$ aperture is further tested. Seal resistances from 12 cells are recorded in cell-attached mode. All cells show $R_{\text{seal}} > 200 \text{ M}\Omega$, 9 cells show $R_{\text{seal}} > 300 \text{ M}\Omega$, and 4 cells show $R_{\text{seal}} > 500 \text{ M}\Omega$. A smaller channel aperture indeed improves seal resistance, which seems to imply that by making an even smaller channel one might be able to obtain R_{seal} in the GigaOhm regime. However, we have shown that a small channel poses problems in forming whole cell patch configuration. This will be discussed in more detail in the next section.

Whole cell patch-clamp measurement

In order to form a whole cell configuration, a CHO cell with Kv2.1 expression is trapped as described in earlier sections. The cell membrane is not broken at this point. After a desirable seal resistance is formed ($>150 \text{ M}\Omega$), a rapid negative pressure is applied on the syringe connecting to the patch channel to break the membrane in the patch area. The whole cell configuration can be confirmed by a drop in the resistance measured and an increase in the capacitance spike in the current response. When the whole cell configuration is obtained, a step voltage is applied from -80 mV to $+60 \text{ mV}$ (the membrane depolarization threshold of Kv2.1 channel is 0 mV), and the current response is recorded. Fig. 5(a), (c) shows the whole-cell current response of two different cells. In the data shown the first cell (Fig. 5(a)) has a whole-cell seal resistance of $161 \text{ M}\Omega$, while the second cell (Fig. 5(c)) has a whole-cell seal resistance of $312 \text{ M}\Omega$. By performing leak subtraction the current passing through the cell membrane is obtained. This is plotted in the $I-V$ curve shown in Fig. 5(b), (d). One important observation from experiments is that a high seal resistance does not make it easier to obtain the whole cell configuration. A small aperture patch channel ($2 \mu\text{m} \times 2 \mu\text{m}$) is used and their ability to form whole cell patch configuration is tested. Out of the 9 cells trapped that are measured with R_{seal} in cell-attached mode to be $>300 \text{ M}\Omega$, only 4 are able to form the whole cell configuration. Not only is it difficult to form the whole cell mode, some of the experiments suffer from cell membrane resealing over time even after the whole cell mode is achieved. On the other hand, for devices with a bigger aperture ($2.5 \mu\text{m} \times 2.5 \mu\text{m}$ or above) it is relatively easier to form the whole cell configuration. Over 80% of the cells trapped with those devices and with R_{seal} in the range $150\text{--}250 \text{ M}\Omega$ are able to form a whole cell configuration. A trick discovered to increase the chance of obtaining the whole cell configuration is to apply rapid pressure to break the membrane in the patch as soon as possible after the cell is trapped. In this way the chance of forming the whole cell mode is increased, but at the expense

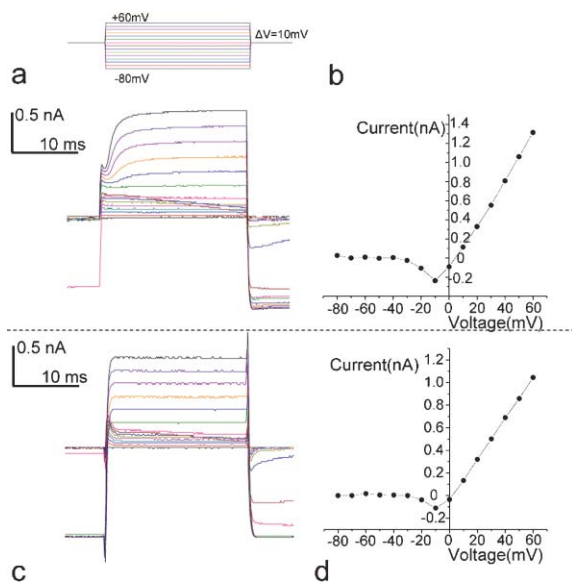


Fig. 5 (a)–(b) The whole-cell current response and the corresponding I–V plot of one experiment. The inset of (a) shows the applied step voltage, which goes from -80 mV to $+60$ mV in 10 mV steps. The current traces in (a) are raw data without any leak subtraction; while the leak current is subtracted for the I–V plot in (b). The whole-cell seal resistance in this data is 161 M Ω . (c)–(d) show similar results as in (a)–(b) but obtained from another experiment. The whole-cell seal resistance in this data is 312 M Ω .

of seal resistance. Capacitive and resistive coupling between different microchannels should be minimal in the set-up because the channels are individually addressable. Even though they share a common reference (at the open chamber), each channel is connected to a different electrode, and measurements are taken on one set of electrodes at a time. This is discussed in previous lateral patch-clamp studies,^{12,13}

Drug response measurement

One advantage of using the open access chamber is that extracellular fluid can be easily exchanged without disturbing the seal quality between the cell and the patch channel. The channel blockage effect of tetraethylammonium (TEA, Sigma) (Kv2.1 channel blocker) on the Kv2.1 expressing CHO cells is observed. A simple perfusion system is set up by using a mechanical syringe pump to flow fluid into the open chamber. A vacuum hose is fixed to the top of the open chamber to remove overflowing fluid. Devices with an aperture geometry of $2.5 \mu\text{m} \times 2.5 \mu\text{m}$ are used. Different concentrations of TEA (2 mM, 5 mM, 10 mM, 20 mM and 50 mM) in buffer solution are flown into the chamber. Before and after the addition of the drug, a step voltage is applied and the current is recorded. If the seal resistance of the patch remains stable after a 1 min, another TEA concentration is flown in and data are recorded. Results are obtained from 9 experiments. Ion channel activity is represented by I/I_{max} , where I_{max} is the magnitude of the current response when no drug is present. Leak subtraction is performed on all the recorded results; the dose–response relationship can be seen in Fig. 6(a). A sigmoidal curve is fitted to the data, and an IC₅₀ (50% inhibitory concentration) of

19.3 mM is obtained. This is relatively close to the value of 13.4 mM reported by Andalib *et al.*¹⁶ A few reasons for the deviations might be as follows: first, data are taken from 9 different experiments from 9 cells, so the variation may result from the different cells; second, the relatively lower seal resistance (compared to the traditional approach in ref. 16) might lead to drug leaking into the cells, affecting intracellular ion channel activity; third, drug adsorption onto the PDMS surface might create a lower local drug concentration.

The drug binding dynamics are observed by measuring current response at different time points when the drug is added and removed. The results can be seen in Fig. 6(b). The results show that the current is almost completely blocked out after 20 mM of TEA is flown in. The current is then restored to about 75% of its initial value when the TEA is washed out.

Conclusions

We present here a novel open-access patch-clamp chip with raised cell trapping microfluidic channels to better resemble

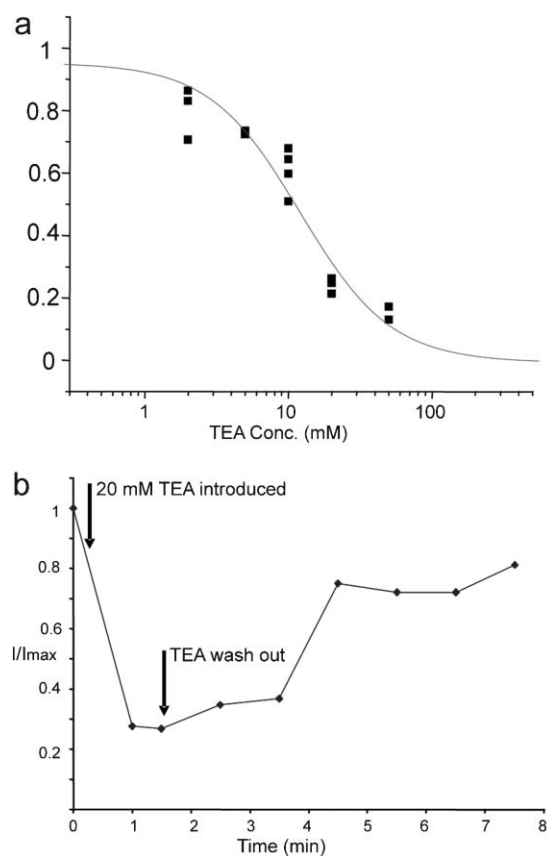


Fig. 6 (a) Dose–response curve of TEA on Kv2.1 expressing cells. Five different concentrations of TEA are used (2 mM, 5 mM, 10 mM, 20 mM and 50 mM). Results are obtained from 9 different experiments. A sigmoidal curve is fitted to the data and an IC₅₀ of 19.3 mM is found. (b) The time dependence of TEA activity by looking at the change in current response over time. Results show that current is partially blocked when TEA is introduced, and also partially restored after TEA is washed out.

traditional glass micropipette openings. The main fluidic chamber is open to the air, providing an easy-to-use platform for fluidic exchange. The smooth surface of open-access patch-clamp sites accomplished by the macroscale hole punching method and seal resistances are characterized. It is shown that a smaller aperture area enhances seal resistance exponentially. However, it is also demonstrated that the higher seal resistance achieved from using small aperture reduces the channel's ability to form a whole cell patch configuration. By balancing the two effects we determined that patch aperture dimensions of (2 μm \times 2 μm) to (2.5 μm \times 2.5 μm) work most effectively in obtaining repeatable seal resistance $\geq 250 \text{ M}\Omega$ with a success rate of forming the whole cell patch configuration $\geq 80\%$. Extensive whole cell patch-clamp experiments are then performed on CHO cells expressing Kv2.1 ion channels, including ion channel I–V characterizations, drug dose–response characterizations, and also dynamic drug activity characterizations. This open-access platform is suitable for high throughput screening of ion channel electrophysiology since it provides easier handling and a shorter data turnaround time compared to the traditional patch-clamp set-up.

Acknowledgements

This work was supported by the National Institutes of Health, the National Science Foundation and the National Aeronautics and Space Administration.

References

- 1 J. Xu, X. B. Wang, B. Ensign, M. Li, L. Wu, A. Guia and J. Q. Xu, *Drug Discovery Today*, 2001, **6**(24), 1278–1287.
- 2 B. Sakmann and E. Neher, *Single Channel Recording*, Plenum, New York, 1983.
- 3 H. J. Neubert, *Anal. Chem.*, 2004, **76**(17), 327A–330A.
- 4 R. Pantoja, J. M. Nagarah, D. M. Starace, N. A. Melosh, R. Blunck, F. Bezanilla and J. R. Heath, *Biosens. Bioelectron.*, 2004, **20**(3), 509–17.
- 5 N. Fertig, A. Tilke, R. H. Blick, J. P. Kotthaus, J. C. Behrends and G. ten Bruggencate, *Appl. Phys. Lett.*, 2000, **77**(8), 1218–1220.
- 6 N. Fertig, M. Klau, M. George, R. H. Blick and J. C. Behrends, *Appl. Phys. Lett.*, 2002, **81**(25), 4865–4867.
- 7 N. Fertig, M. George, M. Klau, C. Meyer, A. Tilke, C. Sobotta, R. H. Blick and J. C. Behrends, *Recept. Channels*, 2003, **9**(1), 29–40.
- 8 A. Stett, V. Bucher, C. Burkhardt, U. Weber and W. Nisch, *Med. Biol. Eng. Comput.*, 2003, **41**(2), 233–40.
- 9 K. G. Klemic, J. F. Klemic, M. A. Reed and F. J. Sigworth, *Biosens. Bioelectron.*, 2002, **17**(6–7), 597–604.
- 10 K. G. Klemic, J. F. Klemic and F. J. Sigworth, *Pfluegers Arch.*, 2005, **449**(6), 564–72.
- 11 Y. N. Xia and G. M. Whitesides, *Annu. Rev. Mater. Sci.*, 1998, **28**, 153–184.
- 12 J. Seo, C. Ionescu-Zanetti, J. Diamond, R. Lal and L. P. Lee, *Appl. Phys. Lett.*, 2004, **84**(11), 1973–1975.
- 13 C. Ionescu-Zanetti, R. M. Shaw, J. G. Seo, Y. N. Jan, L. Y. Jan and L. P. Lee, *Proc. Natl. Acad. Sci. U. S. A.*, 2005, **102**(26), 9112–9117.
- 14 M. Khine, A. Lau, C. Ionescu-Zanetti, J. Seo and L. P. Lee, *Lab Chip*, 2005, **5**(1), 38–43.
- 15 J. G. Trapani and S. J. Korn, *BMC Neurosci.*, 2003, **4**.
- 16 P. Andalib, J. F. Consiglio, J. G. Trapani and S. J. Korn, *Biophys. J.*, 2004, **87**(5), 3148–3161.